

# Determination of Mode I and II Adhesion Toughness of Monolayer Thin Films by Circular Blister Tests

Christopher M. Harvey<sup>1</sup>, Simon Wang<sup>1,2,\*</sup>, Bo Yuan<sup>1</sup>,  
Rachel C. Thomson<sup>3</sup> and Gary W. Critchlow<sup>3</sup>

<sup>1</sup> Department of Aeronautical and Automotive Engineering,  
Loughborough University, Loughborough, Leicestershire LE11 3TU, UK

<sup>2</sup> College of Mechanical and Equipment Engineering,  
Hebei University of Engineering, Handan 056038, China

<sup>3</sup> Department of Materials Engineering,  
Loughborough University, Loughborough, Leicestershire LE11 3TU, UK

**Abstract.** Mechanical models are developed to determine the mode I and II adhesion toughness of monolayer thin films using circular blister tests under the pressure load. The interface fracture of monolayer thin film blisters is mode I dominant for linear bending with small deflection while it is mode II dominant for membrane stretching with large deflection. By taking the advantage of the large mode mixity difference between these two limiting cases, the mode I and II adhesion toughness are determined in conjunction with a linear failure criterion. Thin films under membrane stretching have larger adhesion toughness than thicker films under bending. Experimental results demonstrate the validity of the method.

**Keywords:** adhesion toughness, circular blisters, energy release rate, interface fracture, thin films.

## 1 Introduction

Thin films can detach the substrates by buckling [1–5], pockets of energy concentration [6–8], etc.; therefore, the adhesion toughness of thin films is a major concern in engineering applications. Several experimental techniques have been developed to determine the film's adhesion toughness, such as peeling [9], scratching [10] and blister tests [11–13]. The blister tests are widely used in microelectronics and coating fields. The first blister test was reported by Dannenberg in 1961 [11], which was further developed by Jensen [12,13]. Also, multiple theoretical models have been developed to correlate the adhesion toughness of thin films with the blister morphology [14,15] that is induced by either a pressure load or a point load. Films, such as graphene, and substrates with various material properties and thickness are employed in the blister tests, hence the limits of membrane stretching with large deflections and linear bending with small deflections, and even transition characteristics are necessary in deriving the film's adhesion toughness. Furthermore, the adhesion toughness is influenced by the through-thickness shearing and film sliding [16]. The present work

---

\* Corresponding author, E-mail: s.wang@lboro.ac.uk (Simon Wang)

aims to develop mechanical models to determine the mode I and II adhesion toughness of thin films by using circular blister tests under a pressure load, then the mechanical models are validated with experimental results [17]. Also, the mechanical models for the circular blister test under a point load are developed in Ref. [18].

## 2 Analytical mechanical model for the circular blister test with a pressure load

Figure 1 shows a circular blister under a pressure load  $p$ . The blister radius is  $R_B$  with B denoting the blister tip, and the central deflection is  $\delta$ . The film thickness is  $h$ , which is assumed much smaller than the substrate thickness. Hence, the global deformation of the substrate is negligible. The film's Young's modulus is  $E$  and the Poisson's ratio is  $\nu$ .

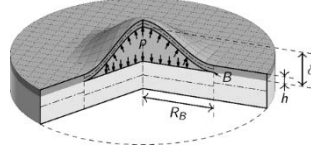


**Fig. 1.** A circular blister test with a thin film under a pressure load on a thick substrate.

### 2.1 Linear bending mechanical model for small deflection

For linear bending limit with small deflections, denoted by the subscript b, the crack tip loads [3–5], i.e. bending moment  $M_B$  ( $\text{Nm m}^{-1}$ ), in-plane force  $N_B$  ( $\text{N m}^{-1}$ ), and through-thickness shear force  $P_B$  ( $\text{N m}^{-1}$ ) are

$$M_{Bb} = \frac{1}{8} p R_B^2, \quad N_{Bb} = 0 \quad \text{and} \quad P_{Bb} = \frac{1}{2} p R_B \quad (1)$$

The mode I and II energy release rates (ERRs) based on 2D partition theories [16,19–21] are,

$$G_I = 0.6227 \times \frac{1}{2} p \delta_b (1 + \lambda)^2 \quad (2)$$

$$G_{II} = 0.3773 \times \frac{1}{2} p \delta_b \quad (3)$$

where  $\delta_b$  is the blister central deflection,

$$\delta_b = \frac{3}{16} \frac{(1 - \nu^2) p R_B^4}{E h^3} \quad (4)$$

and  $\lambda$  represents the through-thickness shear effect,

$$\lambda = \frac{P_{Bb}h}{1.0063M_{Bb}} = \frac{4h}{1.0063R_B} \quad (5)$$

The mode mixity  $\rho$  is readily obtained by Eqs. (2) and (3),

$$\rho = G_{II}/G_I = 0.6059/(1+\lambda)^2 \quad (6)$$

Based on Eqs. (5) and (6), it is found the mode mixity approaches to pure mode I for large  $\lambda$  (or small  $R_B/h$ ), and approaches to 0.6059 for very small  $\lambda$ . In addition, the total ERR can be given by combining Eqs. (2) and (3) and expressed by

$$G = G_j + G_s = G_j(1 + G_s/G_j) = G_j[1 + 0.6227\lambda(2 + \lambda)] \quad (7)$$

where  $G_j = 1/(2p\delta_b)$  is the ERR component from Jensen's work [3–5], which does not account for through-thickness shear; but  $G_s$  demonstrates the ERR component due to the crack tip through-thickness shear force  $P_{Bb}$ . It is seen that the through-thickness shear tends to decrease the mode mixity shown by Eq. (6) and consequently to reduce the adhesion toughness, as per Eq. (7).

## 2.2 Membrane stretching mechanical model for large deflection

For membrane stretching limit with large deflections, denoted by the subscript m, the crack tip loads [3–5] in Eq. (1) become

$$M_{Bm} = \frac{h}{4} \frac{(Ehp^2R_B^2)^{1/3}}{[3(1-\nu^2)\phi(\nu)]^{1/2}}, \quad N_{Bm} = (Ehp^2R_B^2)^{1/3}\phi(\nu) \quad \text{and} \quad P_{Bm} = \frac{1}{2}pR_B \quad (8)$$

where the parameter  $\phi(\nu)$  is

$$\phi(\nu) = \frac{(1.078 + 0.636\nu)^{2/3}}{2[6(1-\nu^2)]^{1/3}} \quad (9)$$

The blister central deflection becomes

$$\delta_m = 0.9635 \left[ \frac{3(1-\nu)}{7-\nu} \right]^{1/3} \left( \frac{pR_B^4}{Eh} \right)^{1/3} \quad (10)$$

The mode I and II ERRs [16,19–21] are

$$G_I = 0.6227 \times \frac{p\delta_m}{8} \frac{(0.7578 - 0.1429\nu)^2}{\phi(\nu)f(\nu)} \quad (11)$$

$$G_{II} = 0.3773 \times \frac{p\delta_m}{8} \frac{(1.400 + 0.2358\nu)^2}{\phi(\nu)f(\nu)} \quad (12)$$

Hence, the total ERR is

$$G = \left[ \frac{1}{8\phi(\nu)} + \frac{(1-\nu^2)\phi(\nu)^2}{2} \right] \frac{\rho\delta_m}{f(\nu)} \quad (13)$$

and the mode mixity for membrane stretching with large deflection is

$$\rho = 0.6059 \left( \frac{1.400 + 0.2358\nu}{0.7578 - 0.1429\nu} \right)^2 \quad (14)$$

Eq. (14) shows that  $\rho$  varies from 2.0680 for  $\nu = 0$  to 2.9634 for  $\nu = 0.5$ , and remains constant during blister radial growth. The adhesion toughness  $G_c$  therefore remains constant with mode II dominant, and consequently it is expected to be larger than the adhesion toughness of films under linear bending.

Now, the linear failure criterion is used to derive the mode I and II adhesion toughness, which is considered as an accurate failure criterion for interfaces with low adhesion toughness [6,7,16,22,23]. For any given mode mixity  $\rho$ , the corresponding adhesion toughness  $G_c$  is

$$G_c = \frac{(1+\rho)G_{lc}G_{llc}}{\rho G_{lc} + G_{llc}} \quad (15)$$

Based on Eq. (15), by choosing two values of mode mixities, with their corresponding adhesion toughness, the mode I and II adhesion toughness can be readily obtained. But, when used in conjunction with linear bending model, more accurate predictions for  $G_{lc}$  and  $G_{llc}$  can be determined than from using just the linear bending model alone. Hence, by choosing  $\rho_b$  and  $\rho_m$ , with  $G_{cb}$  and  $G_{cm}$ , the mode I and II adhesion toughness can be obtained as

$$G_{lc} = \frac{G_{cb}G_{cm}(\rho_b - \rho_m)}{\rho_b G_{cb}(1 + \rho_m) - \rho_m G_{cm}(1 + \rho_b)} \quad (16)$$

$$G_{llc} = \frac{G_{cb}G_{cm}(\rho_b - \rho_m)}{G_{cm}(1 + \rho_b) - G_{cb}(1 + \rho_m)} \quad (17)$$

### 3 Experimental validation

The mechanical models developed above are validated using the experimental results as presented in Ref. [17]. In the first experiment group, photoresist films with three different thickness  $h$  are blistered from the copper substrate with a thickness of 80  $\mu\text{m}$ , under a pressure load. The film's Young's modulus is 3.6 GPa and the Poisson's ratio is 0.35. The Young's modulus of copper is about 128 GPa, which is much larger than that of the photoresist films. Therefore, the present thin film models are still applicable. Based on the comparison between the predicted and experimental adhe-

sion toughness, it is found that  $h = 10 \mu\text{m}$  corresponds to membrane stretching limit, and both  $h = 31 \mu\text{m}$  and  $h = 60 \mu\text{m}$  correlates to linear bending limit. The predictions of the adhesion toughness based on the analytical model are summarised in Table 1.

**Table 1.** Analytical predictions of the adhesion toughness for various film thickness.

Thickness ( $\mu\text{m}$ )	Mode mixity ( $\rho = G_{II}/G_I$ )	Measured adhesion Toughness ( $\text{J m}^{-2}$ )	Mode I Toughness ( $\text{J m}^{-2}$ )	Mode II Toughness ( $\text{J m}^{-2}$ )
Photoresist/copper				
10	2.6583 Eq. (14)	0.3487 Eq. (13)		
31	0.5189 Eq. (6)	0.2827 Eq. (7) [0.2845 Eq. (15)]	0.2446 Eq. (16)	0.4152 Eq. (17)
60	0.4535 Eq. (6)	0.2805 Eq. (7)		
Photoresist-graphene/copper				
10	2.6583 Eq. (14)	0.4435 Eq. (13)		
31	0.5189 Eq. (6)	0.3711 Eq. (7) [0.3710 Eq. (15)]	0.3240 Eq. (16)	0.5149 Eq. (17)
60	0.4535 Eq. (6)	0.3664 Eq. (7)		

First, the mode mixities and the corresponding adhesion toughness at  $R_B = 1530 \mu\text{m}$  for  $h = 10 \mu\text{m}$  and  $h = 60 \mu\text{m}$  are determined by Eqs. (13) and (14), and Eqs. (6) and (7), respectively. Then, the film's mode I and mode II adhesion toughness can be determined with the mode mixities and the corresponding adhesion toughness at for thickness  $10 \mu\text{m}$  and  $60 \mu\text{m}$  by Eqs. (16) and (17). Next, substituting  $G_{Ic}$ ,  $G_{IIc}$  and  $\rho$  for thickness  $31 \mu\text{m}$  into Eq. (15) gives the analytical  $G_c = 0.2845 \text{ J m}^{-2}$ , which is in excellent agreement with the experimental result shown in Table 1.

In the second experiment group, a monolayer graphene is sandwiched between the photoresist films and the copper substrate. The thickness of the monolayer graphene is about  $0.347 \text{ nm}$  [16]. Even considering the Young's modulus of the graphene is about  $1000 \text{ GPa}$ , its effective thickness is still much smaller than the thickness of the photoresist films and it is therefore ignored in the present work. The addition of the graphene layer, however, changes the adhesion toughness at the interface. Following the same analytical procedure as that for the first group, the analytical predictions are summarised in Table 1. It is seen again the analytical adhesion toughness  $G_c = 0.3710 \text{ J m}^{-2}$  for  $h = 31 \mu\text{m}$  is in excellent agreement with the experimental result shown in Table 1.

## 4 Conclusions

This work shows the mechanical models for circular blister tests under a pressure load. The large mode mixity difference between the limits of membrane stretching and linear bending enables the mode I and II adhesion toughness of thin films to be accurately determined, which can be well validated with experimental results. For linear bending with small deflection, the interface fracture of thin film blisters is mode I dominant. The through-thickness shear force makes an extra contribution to the mode I ERR and decreases the mode mixity. The thicker the film is, the smaller the adhesion toughness is. For membrane stretching with large deflection, the inter-

face fracture is mode II dominant. Membrane films consequently have larger adhesion toughness. Furthermore, the through-thickness shear force has no effect on the mode mixity which is only dependent on the Poisson's ratio. In addition, the mechanical models for circular blister tests under a point load are developed in Ref. [18].

## References

1. Chai, H.: Three-dimensional fracture analysis of thin-film debonding. *Int. J. Fract.* 46(4), 237–256 (1990).
2. Hutchinson, J.W., Thouless, M.D., Liniger, E.G.: Growth and configurational stability of circular, buckling-driven film delaminations. *Acta Metall. Mater.* 40(2), 295–308 (1992).
3. Jensen, H.M., Sheinman, I.: Straight-sided, buckling-driven delamination of thin films at high stress levels. *Int. J. Fract.* 110(4), 371–385 (2001).
4. Moon, M.W., Jensen, H.M., Hutchinson, J.W., Oh, K.H., Evans, A.G.: The characterization of telephone cord buckling of compressed thin films on substrates. *J. Mech. Phys. Solids.* 50(11), 2355–2377 (2002).
5. Jensen, H.M., Sheinman, I.: Numerical analysis of buckling-driven delamination. *Int. J. Solids Struct.* 39(13–14), 3373–3386 (2002).
6. Wang, S., Harvey, C.M., Wang, B.: Room temperature spallation of  $\alpha$ -alumina films grown by oxidation. *Eng. Fract. Mech.* 178, 401–415 (2017).
7. Harvey, C.M., Wang, B., Wang, S.: Spallation of thin films driven by pockets of energy concentration. *Theor. Appl. Fract. Mech.* 92, 1–12 (2017).
8. Yuan, B., Harvey, C.M., Thomson, R.C., Critchlow, G.W., Wang, S.: Telephone cord blisters of thin films driven by pockets of energy concentration. In review.
9. Kendall, K.: Thin-Film Peeling - The Elastic Term. *J. Phys. D. Appl. Phys.* 8(13), 1449–1452 (1975).
10. Akono, A.T., Ulm, F.J.: An improved technique for characterizing the fracture toughness via scratch test experiments. *Wear.* 313(1–2), 117–124 (2014).
11. Dannenberg, H.: Measurement of adhesion by a blister method. *J. Appl. Polym. Sci.* 5(14), 125–134 (1961).
12. Jensen, H.M.: Analysis of mode mixity in blister tests. *Int. J. Fract.* 94(1), 79–88 (1998).
13. Jensen, H.M.: The blister test for interface toughness measurement. *Eng. Fract. Mech.* 40(3), 475–486 (1991).
14. Malyshev, B.M., Salganik, R.L.: The strength of adhesive joints using the theory of cracks. *Int. J. Fract. Mech.* 1(2), 114–128 (1965).
15. Wang, Y., Tong, L.: Closed-form Formulas for Adhesion Energy of Blister Tests Under Pressure and Point Load. *J. Adhes.* 92(3), 171–193 (2016).
16. Wood, J.D., Harvey, C.M., Wang, S.: Adhesion toughness of multilayer graphene films. *Nat. Commun.* 8(1), 1952 (2017).
17. Cao, Z., Tao, L., Akinwande, D., Huang, R., Liechti, K.M.: Mixed-mode traction-separation relations between graphene and copper by blister tests. *Int. J. Solids Struct.* 84, 147–159 (2016).
18. Harvey, C.M., Wang, S., Yuan, B., Thomson, R.C., Critchlow, G.W.: Determination of mode I and II adhesion toughness of monolayer thin films by circular blister tests. *Theor. Appl. Fract. Mech.* In press.
19. Wood, J.D., Harvey, C.M., Wang, S.: Partition of mixed-mode fractures in 2D elastic orthotropic laminated beams under general loading. *Compos. Struct.* 149, 239–246 (2016).
20. Harvey, C.M., Wood, J.D., Wang, S., Watson, A.: A novel method for the partition of mixed-mode fractures in 2D elastic laminated unidirectional composite beams. *Compos. Struct.* 116(1), 589–594 (2014).
21. Hutchinson, J.W., Suo, Z.: Mixed Mode Cracking in Layered Materials. In: *Advances in Applied Mechanics.* 63–191 (1991).
22. Harvey, C.M., Wang, S.: Experimental assessment of mixed-mode partition theories. *Compos. Struct.* 94(6), 2057–2067 (2012).
23. Harvey, C.M., Eplett, M.R., Wang, S.: Experimental assessment of mixed-mode partition theories for generally laminated composite beams. *Compos. Struct.* 124(C), 10–18 (2015).